Sensors and Materials, Vol. 34, No. 8 (2022) 3229–3239
MYU Tokyo

S & M 3037

Development of Oil Film Thickness Measurement Software Using Optical Interferometry

Li-Ming Chu,[1] Chia-Wei Lee,[2] Hsiang-Chen Hsu,[3*]
Chi-Yu Liu,[2] Tun-hao Li,[1] and Shou-Cheng Hsiung[3]

[1]Interdisciplinary Program of Green and Information Technology, National Taitung University,
No. 369, Sec. 2, University Rd., Taitung City 95092, Taiwan, R.O.C.
[2]Department of Computer Science, National Taitung University,
No. 369, Sec. 2, University Rd., Taitung City 95092, Taiwan, R.O.C.
[3]Department of Industrial Management, I-Shou University,
No. 1, Sec. 1, Syucheng Rd., Dashu District, Kaohsiung City 84001, Taiwan, R.O.C.

(Received February 25, 2022; accepted July 13, 2022)

Keywords: film thickness measurement software (FTMS), optical interferometry, elastohydrodynamic lubrication (EHL), squeeze speed control system (SSCS)

In this study, C# programming language on the Visual Studio platform and a novel algorithm were used to develop software for the calculation and analysis of the oil film thickness distribution. The execution of the software is divided into file reading, conversion to grayscale values, inputting coordinates or drawing a line manually, and data acquisition. This software also provides the grid auxiliary function, the storage of the original image, the storage of the grayscale versus pixel graph, and the storage of data functions. After grayscale data are obtained from the above steps, they will be drawn into a line chart. The changes in bright and dark fringes can be clearly distinguished from the grayscale image, and the film thickness is calculated using the interference equation. In this study, we used an optical elastohydrodynamic lubrication (EHL) impact tester and the self-developed film thickness measurement software (FTMS) to measure the dimple film thickness occurring when a ball impacts a flat plate covered with a thin layer of oil for different operation parameters. Excellent agreement between the value determined with FTMS and that determined with the commercial software has been reported after a series of comprehensive experiments.

1. Introduction

Owing to the squeeze effect, a high pressure will be generated in a lubricated film and an elastic dimple will be formed at the center of a contact region. These phenomena occur in many mechanical components.

Optical interferometry is a widely used technique for measuring oil film thickness in rolling and sliding elastohydrodynamic lubrication (EHL) contacts. Cameron and Gohar[(1)] firstly used optical interferometry to measure the film thickness of an EHL point contact. Many experimental

*Corresponding author: e-mail: hchsu@isu.edu.tw
https://doi.org/10.18494/SAM3875

ISSN 0914-4935

methods including the semi-reflective chromium layer technique,[2] spacer layer technique,[3] ultrathin film interferometry (UTFI) technique,[4] the lubricated impact using optical interferometry,[5] and the spacer layer mapping (SLM) technique[6] have been proposed to improve clarity and accuracy for the measured oil film in EHL contact problems.

Optical interferometry can be used to measure accurately and efficiently oil film thickness using modern image analysis software. Gustafsson *et al.*[7] matched the hue in a digital color interferometer image of an unknown film shape with the calibration value to obtain the film thickness. Lord *et al.*[8] presented the multichannel method to measure film thickness and overcome error problems. Furthermore, Hartl *et al.*[9] presented colorimetric interferometry combining conventional chromatic interferometry with image processing and differential colorimetry to determine the instantaneous film thickness distribution on EHL. Wong *et al.*[10] presented the surface plasmon resonance (SPR) for the measurement of the refractive index[11] profile in EHL dimples. Marx *et al.*[12] used the conventional optical interferometry technique to map film thickness in soft-EHL contacts and developed film thickness equations for soft-EHL conditions. Yagi *et al.*[13] used optical interferometry and the infrared emission technique to elucidate the mechanism of EHD lubricated oil film changes for high slip ratio and temperature difference. Zhang and Glovnea[14] used the UTFI and SLM techniques to measure the film thickness profile on the EHL point contact and determine the behavior of grease-lubricated film for variable loading.

It is expensive to buy and maintain a commercial image analysis software package. The operating system must be maintained and upgraded every year. Therefore, in this study, we used an optical EHL impact device and self-developed software to explore the EHL dimple at impact squeeze loading. We wrote the software by using the C# programming language and a novel algorithm. This self-developed software is used to calculate and analyze the oil film thickness distribution, and it can be independently modified to incorporate new functions.

2. Theoretical Analysis

A digital image is an image composed of picture elements, also known as pixels. A pixel in a monochrome or gray-level image is the value of two-dimensional functions $f(x, y)$ indicating its intensity or brightness. x and y are its spatial coordinates on the x- and y-axes, respectively. In a monochrome image, brightness is called gray level. This is why we also call a monochrome image a gray-level image. Therefore, we use a two-dimensional array to represent a digital image. The elements in the two-dimensional array are the values of pixels, and the column and row represent the x- and y-axes, respectively.

Digital image processing is the use of a digital computer to process digital images through an algorithm. The operations between pixels can be divided into three levels according to the range of effects. These three levels are point operation, local operation, and global operation. In this study, our image processing level is point operation, in which the pixels are processed pixel by pixel. That is, each pixel is processed independently.

The human eye is sensitive to three primary colors, namely, red, green, and blue (RGB), and it is more sensitive to the green and red components than to the blue component. When converting from an RGB color image to a grayscale image, we need to give different weights to these three

primary colors. The reason for this is to consider the characteristics of the original RGB image, and it can also be close to the perception of the human eye. In the developed software, we use the following conversion formula for each pixel:[15]

$$\text{grayscale value} = \text{red value} \times 0.299 + \text{green value} \times 0.587 + \text{blue value} \times 0.114. \quad (1)$$

We use the basic three-step process algorithm shown as follows to convert grayscale values. With the converting algorithm, we perform the following:[16] 1. Get the red, green, and blue values of each pixel; 2. use the formula shown above to turn these values into a single gray value; 3. replace the original red, green, and blue values with the new gray value calculated in step 2.

The oil film thickness can be quickly determined using the relationship formula of optical interference that can be described as

$$m\lambda = 2nh,\ m = 0, 1, 2, \ldots \quad (2)$$

Moreover, according to the principle of refraction, the refractive indexes of the different mediums need to be expressed as

$$n_1 h_1 = n_2 h_2, \quad (3)$$

where m is the number of Newton's rings, λ is the wavelength of incident light, n is the refractive index, and h is the oil film thickness.

3. Experimental Apparatus and Method

The contact area between two mechanical components is measured in micrometer, whereas the oil film thickness between them is measured in nanometer. Considerable technical difficulties are inevitably encountered when measuring a complicated lubrication phenomenon in such a tiny space. As common mechanical measurement methods are not suitable for the measurement of the oil film thickness in a tiny space, a nonmechanical measurement technology is required.

The distribution of the oil film (paraffin-based oil) in an EHL point contact is explored by optical interferometry. Figures 1(a) and 1(b) show the device scheme[17] and a photo of the experimental hardware, respectively. The oil film exists between the gap of the sapphire glass disk and the steel ball. The sapphire glass disk is coated with a semi-reflecting chromium layer and a silica spacer layer. All the material parameters are summarized in Table 1.

The steel ball was delivered towards the optical glass plate through a bar that drops under loading. The squeeze speed control system (SSCS) determines the ball access speed. This system consists of a DC motor, screws, and gears in order to change the motion direction and control the access speed. When the weight leaves the SSCS, the steel ball is installed on the optical glass disc. A noncontact displacement transducer was installed between the optical glass plate and the steel ball in order to measure precisely the displacement of the steel ball during extrusion motion. A micrometer was used to adjust the different mounting positions.

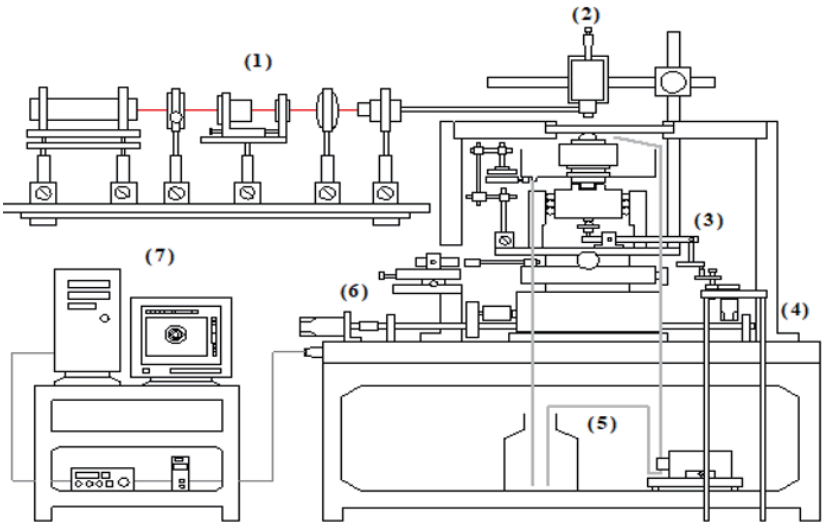

(a)

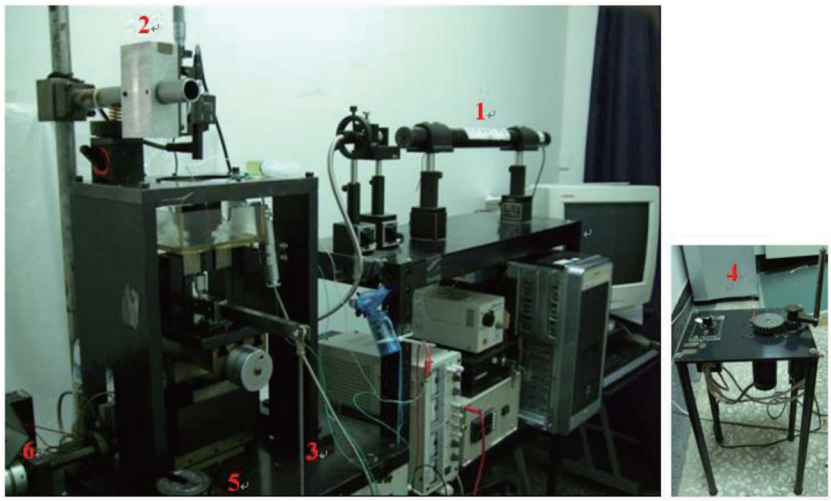

(b)

Fig. 1. (Color online) EHL squeeze device with optical interferometry equipment. (a) Schematic illustration of self-developed measurement system and (b) photo of optical interferometry experimental system. (1) He-Ne laser, (2) charge-coupled device (CCD) camera recording, (3) applied load system, (4) SSCS, (5) oil supply system, (6) sliding speed control system, (7) data acquisition, management, and analysis system.

Table 1
Characteristics of optical glass disc and steel ball.

	Optical Glass Disc	Steel Ball
Modulus of elasticity (Pa), *E*	74.5 × 109	207 × 109
Poisson ratio, *v*	0.23	0.30
Surface roughness, *ms* (m)	0.0038	0.0372
Diameter (mm)	150	50
Thickness (mm)	12	—
Type of disc coating	120 chrome layer	—

The light source was a He-Ne laser of 632.8 mm wavelength. Through the bright optical glass disc, the interference fringe patterns of the contact region were observed by CCD camera recording using optical interferometry. The schematic of the optical interferometry equipment is shown in Fig. 2.

The laser light illuminated vertically, so the refraction angle was 90°. The oil film thickness was determined using Eqs. (2) and (3). We took a picture of a steel wire of 0.602 mm diameter and used commercial software (Matrox Inspector) to analyze the steel wire diameter relative to the pixel size as shown in Fig. 3. Furthermore, the actual width per pixel was calculated ($0.602/291=2.069\cdot10^{-3}$ mm/pixel). A constant speed of 1.0–2.0 mm/s was applied to both solids. The ball was pressed against the disk with a load of 82.6–155.9 N; thus, the maximum pressure according to the Hertz theory was 0.871 GPa. The lubricants were low-viscosity (LN) oil and high-viscosity (HN) oil. The experimental conditions of speed, load, and oil viscosity are summarized in Table 2.

4. Results and Discussion

In this study, C# programming language on the Visual Studio platform and a novel algorithm were used to write the software for the calculation and analysis of the oil film thickness distribution. Some 2D and 3D figures were drawn by using the date from the self-developed software.

4.1 Optical interferometry

According to the principle of optical interference, if the incident light is monochromatic and the incident direction of the light analyzed is perpendicular to the film, the oil film thickness difference between two adjacent bright or dark fringes in the interference fringe image (where the phase difference is equal to 2π) is equal to half the wavelength of light in the oil film. Moreover,

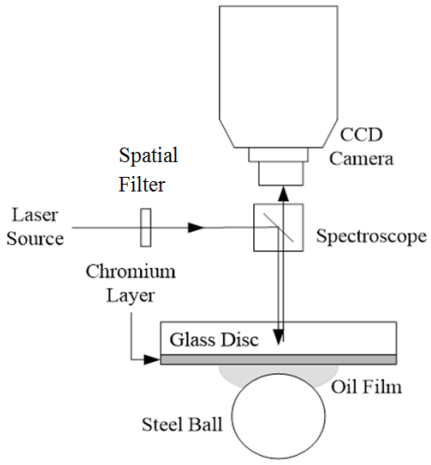

Fig. 2. Schematic of optical interferometry equipment.

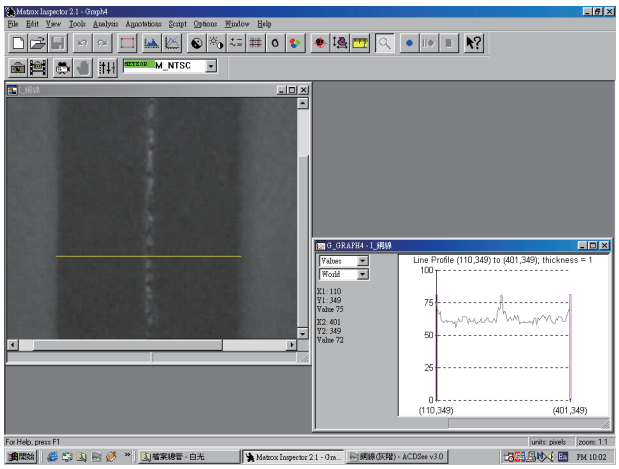

Fig. 3. (Color online) Resolution correction diagram using Matrox Inspector.

Table 2
Experimental parameters and conditions.

Experimental parameter	Experimental Condition
Lubricant viscosities	HN (high-viscosity) oil
	LN (low-viscosity) oil
Radius (mm)	25
Squeeze speed (mm/s)	1
	2
Load (N)	82.6
	155.9

the refractive indexes of the different mediums need to be considered according to the principle of refraction.

Figures 4(a) and 4(b) show the interference fringe patterns of the contact region. The red and black interference fringe picture (pattern) is measured using a He-Ne laser. Then, the grayscale interference fringe picture is interpreted and analyzed using the image analysis software. Finally, the pixel intensity values of the interference fringe image are represented by numbers ranging from 0 to 255, where 0 represents black, 255 represents white, and the others are coded in grayscale gradient values. As mentioned above, the oil film thickness difference between two adjacent bright fringes in the interference fringe image is equal to half the wavelength of light. This experiment uses He-Ne laser light with a wavelength of 632.8 nm to measure the HN oil product with a refractive index of 1.48. Therefore, the measured oil film thickness is 213.8 nm between the bright (or black) fringes. If the interference fringe pattern is less than a circle in the central region, then the oil film thickness can be calculated with the grayscale value using the image analysis software. The oil film thickness between the two bright fringes is $h_1 = n_2 h_2 / n_1$. The minimum measurable film thickness is also about 10 nm.

The calculation time of the color picture is long owing to the three primary colors of RGB. The grayscale color mode can only provide primary colors of black and white; however, there are 256 gradient values between black and white, and only 7 bits are used by each pixel to record data, so the data are far less than that of the RGB mode, which makes it easier and faster to process and analyze the data.

4.2 Film thickness measurement software (FTMS)

FTMS is developed on the Visual Studio platform using the C# programming language, and the interface of the activated software is shown in Fig. 5. The left side of the interface is the function key area, and the right side of the interface is the area to show related data. The execution of the software is divided into the following four steps:

(1) File reading: The software first reads the image to be analyzed. After the "Open Image" button is pressed, the image to be analyzed can be selected, and the read image is displayed in area A.
(2) Conversion to grayscale values: The grayscale formula is used to convert the read image to the grayscale values. After the "Convert to grayscale values" button is pressed, the original image will be gray-scaled and plotted in area A.

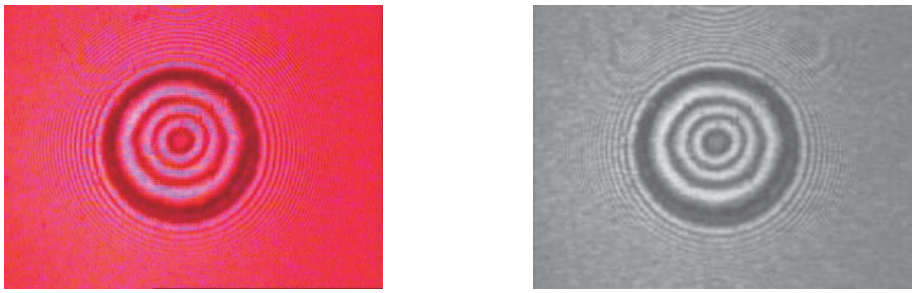

(a) (b)

Fig. 4. (Color online) (a) Measured interference fringe and (b) interpreted grayscale interference fringe patterns.

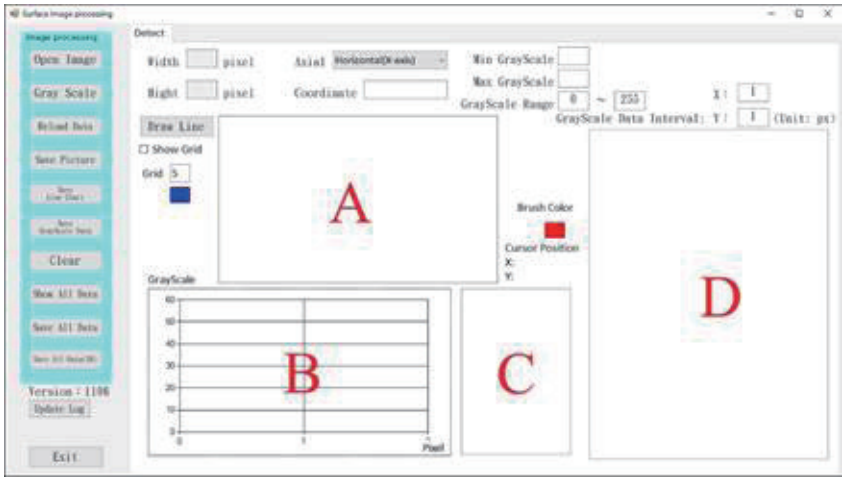

Fig. 5. (Color online) Developed FTMS interface.

(3) Input coordinates or draw line manually: Next, the user may draw lines directly on the analyzed graph or enter the coordinate data manually with respect to the analyzed part (coordinate).
(4) Data acquisition: After completing the previous steps, the user may click "Update Data" and the software will obtain the grayscale values of the line segment and display them in area C. Moreover, the grayscale values of the line segment will also be plotted in area B. After the "Show All Data" button is pressed, the grayscale values of the whole image can be calculated and displayed in area D.

In addition to the above-mentioned basic functions, the developed FTMS also provides other functions as described below. When drawing a line, the user can activate the auxiliary grid to help draw the lines. The lines and grid colors can be adjusted according to the user's preference for easy observation. After the software is executed, the demanded results displayed on the screen are shown in Fig. 6. As can be seen, the measured interference fringe patterns of the contact region are read and converted to the gray-scaled interference fringe patterns, a horizontal line is drawn (coordinate 219) to analyze the data, and the grayscale values of the line segment are plotted and displayed.

4.3 Experimental results

Figure 7 shows that the oil dimple thickness of the contact region obtained using FTMS is comparable to that obtained using the commercial software, Matrox Inspector[17] with experimental conditions of 82.602 N, 1 mm/s, and the HN lubricant. The interference fringe patterns of the contact region are also demonstrated. It is reported that the discrepancies are less than 5% and excellent agreement is found.

Figure 8 shows the oil dimple depth of the contact region using present software (FTMS) with 82.60 2N and the HN lubricant for different squeeze speeds. It can be seen that the dimple depth becomes deeper as squeeze speed increases. The momentum increases as squeeze speed increases. The greater the squeeze speed, the greater the elastic deformation.

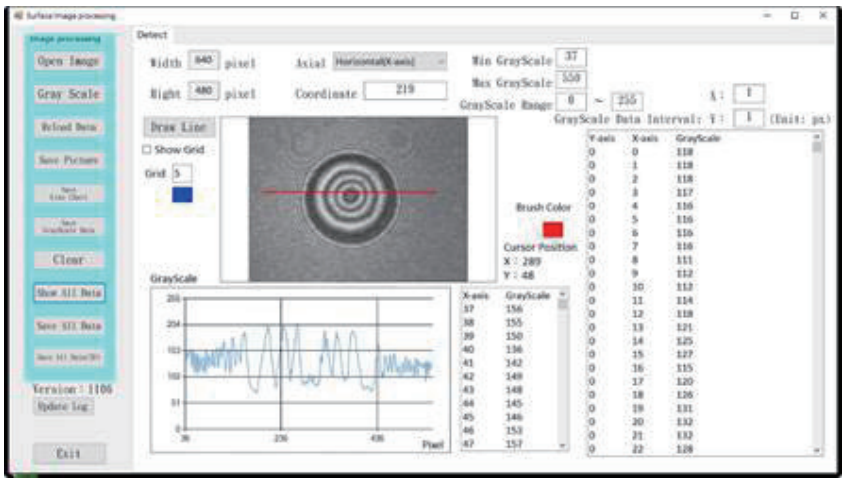

Fig. 6. (Color online) Execution results on FTMS display window.

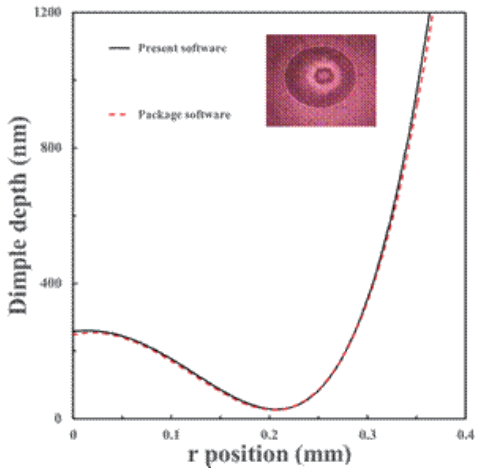

Fig. 7. (Color online) Comparison of oil film shape obtained using FTMS with that obtained using package software (Matrox Inspector).

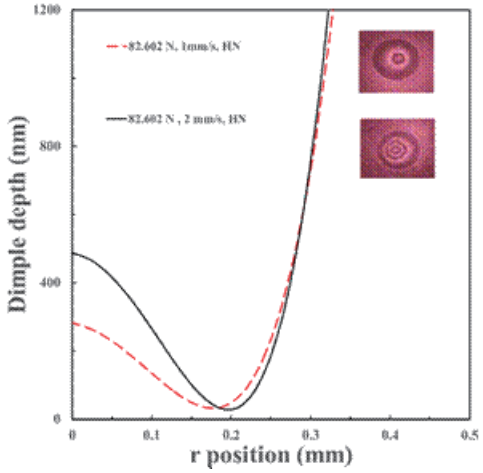

Fig. 8. (Color online) Dimple depth based on interference fringe patterns for different squeeze speeds obtained using FTMS.

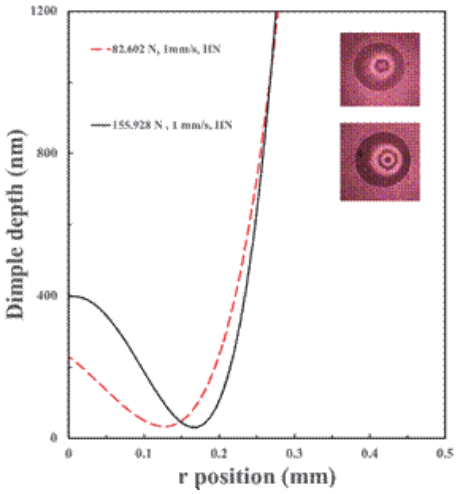

Fig. 9. (Color online) Dimple depth based on interference fringe patterns for different loads obtained using FTMS.

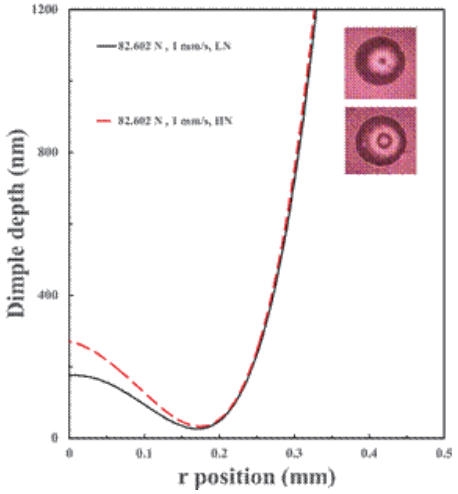

Fig. 10. (Color online) Dimple depth based on interference fringe patterns for different lubricant viscosities obtained using FTMS.

Figure 9 shows the oil dimple depth of the contact region obtained using FTMS with 1 mm/s and the HN lubricant for different loads. The number of Newton's rings increases, so the dimple depth increases. The impact force increases with the load. The larger load results in a greater elastic deformation. The dimple depth also increases with the load.

Figure 10 shows the oil dimple depth of the contact region obtained using FTMS with 82.602 N and 1 mm/s for different lubricant viscosities. The number of Newton's rings increases with the lubricant viscosity. The lubricant viscosity increases as the lubricant fluidity decreases. Therefore, the dimple depth increases with the lubricant viscosity.

5. Conclusions

In this study, C# programming language on the Visual Studio platform and a novel algorithm were used to write the software for the calculation and analysis of the oil film thickness distribution. In this study, we used an optical EHL impact device and FTMS to investigate the effects of extrusion speed, load, and lubricant viscosity on the dimple film thickness due to squeeze motion. The oil dimple thickness of the contact region obtained using FTMS is comparable to that obtained using commercial software with 82.602 N, 1 mm/s, and the HN lubricant. The discrepancies are less than 5%. The usefulness of the optical interferometry technique for measuring the oil film thickness in rolling and sliding EHL contacts has been revealed in this paper.

Acknowledgments

The authors would like to express their appreciation to the Ministry of Science and Technology (MOST 108-2221-E-143-006) of Taiwan, R.O.C. for financial support.

References

1 A. Cameron and R. Gohar: Proc. Math. Phys. Eng. Sci. **291** (1966) 520.
2 D. Choudhury, D. Rebenda, S. Sasaki, P. Hekrle, M. Vrbka, and M. Zou: J. Mech. Behav. Biomed. Mater. **81** (2018) 120.
3 R. Kapadia, R. Glyde, and Y. Wu: Tribol. Int. **40** (2007) 1667.
4 G. J. Johnston, R. Wayte, and H. A. Spikes: Tribol. Trans. **34** (1991) 187.
5 R. Larsson and J. Lundberg: Wear **190** (1995) 184.
6 P. M. Cann, H. A. Spikes, and J. Hutchinson: Tribol. Trans. **39** (1996) 915.
7 L. Gustafsson, E. Hoglund, and O. Marklund: P. I. Mech. Eng. J-Eng. **208** (1994) 199.
8 J. Lord, O. Marklund, and R. Larsson: Tribol. Series **38** (2000) 711.
9 M. Hartl, I. Krupka, R. Poliscuk, and M. Liska: Tribol. Trans. **42** (1999) 303.
10 C. L. Wong, H. P. Ho, K. S. Chan, P. L. Wong, S. Y. Wu, and C. Lin: Tribol. Int. **41** (2008) 356.
11 P. L. Wong, F. Guo, and C. Feng: Tribol. Int. **36** (2003) 497.
12 N. Marx, J. Guegan, and H. A. Spikes: Tribol. Int. **99** (2016) 267.
13 K. Yagi, K. Kyogoku, and T. Nakahara: P. I. Mech. Eng. J-Eng. **220** (2006) 353.
14 X. Zhang and R. Glovnea: Tribol. Int. **147** (2020) 106272.
15 M. Ahmad, Z. Abbas, A. Nasir, M. Waseem, A. Azim, and A. Abbas: Int. J. Comput. Sci. Eng. **8** (2019) 316.
16 G. Jyothi, C. H. Sushma, and D. S. S. Veeresh: Int. J. Comput. Sci. Inf. Technol. Res. **3** (2015) 279.
17 L. M. Chu, J. R. Lin, and Y. P. Chang: Key Eng. Mater. **739** (2017) 164.

About the Authors

Li-Ming Chu received his Ph.D. degree in mechanical and electro-mechanical engineering from National Sun Yat-Sen University, Taiwan. He worked for KYMCO as an engineer in the R & D Center from 1994 to 1999. Currently, he is a full professor in the Interdisciplinary Program of Green and Information Technology, National Taitung University. Taiwan. His research interests are in optical measurement, tribology, hydrogen-gasoline compound power, vehicle engineering, and inverse problems.

Chia-Wei Lee received his B.S. and M.S. degrees from the Department of Computer Science and Information Engineering of National Chi Nan University, Taiwan, in 2003 and 2005, respectively, and his Ph.D. degree from the Department of Computer Science and Information Engineering, National Cheng Kung University, Tainan, Taiwan, in 2009. He then served the compulsory 11-month military service. From December 2011 to July 2017, he was an assistant research fellow at the Department of Computer Science and Information Engineering, National Cheng Kung University. In 2017, he joined the Department of Computer Science and Information Engineering, National Taitung University, and he is now an associate professor. His current research interests include graph theory and algorithms, interconnection networks, and system-level diagnosis.

Hsiang-Chen Hsu received his B.S. degree from National Cheng Kung University, Taiwan and his M.S. and Ph.D. degrees from North Carolina State University, USA. After graduation, he was an associate professor and then became a full professor at I-Shou University, Taiwan. He was the vice president of St. John's University in Taiwan from 2017 to 2019. Currently, he is a full professor jointly appointed by the Department of Industrial Management and the Department of Mechanical and Automation Engineering, I-Shou University. His research interests are in IC packaging, smart automation, pattern recognition, and industrial analysis.

Chi-Yu Liu received his B.S. degree from the Department of Computer Science and Information Engineering of National Taitung University, Taitung, Taiwan, in 2021. He is currently working toward his M.S. degree in the same department. His current research interests include the design and analysis of algorithms.

Tun-Hao Li received his B.S. and M.S. degrees from the Department Applied of Science of National Taitung University, Taitung, Taiwan, in 2019 and 2021, respectively. His current research interests include image analysis research and computer fluid dynamics.

Shou-Cheng Hsiung received his B.S. degree from the Department of Industrial Engineering and Management, Chung Yuan Christian University, Taiwan, in 1995 and his M.S. degree from the Institute of Resources Management, National Defense University, Taiwan, in 2005. Currently, he is a colonel in the Army Logistics Command, ROC, as well as a Ph.D. candidate in the Department of Industrial Management of I-Shou University. His research interests are in AI human resource management, metaheuristics algorithm, and image recognition.